

## Floquet analysis of atom-optics tunneling experiments

Robert Luter and L. E. Reichl

*Center for Studies in Statistical Mechanics and Complex Systems, The University of Texas at Austin, Austin, Texas 78712*

(Received 1 May 2002; published 18 November 2002)

Dynamical tunneling has been observed in atom-optics experiments by two groups. We show that the experimental results are extremely well described by time-periodic Hamiltonians with momentum quantized in units of the atomic recoil. The observed tunneling has a well-defined period when only two Floquet states dominate the dynamics. Beat frequencies are observed when three Floquet states dominate. We find frequencies that match those observed in both experiments. The dynamical origin of the dominant Floquet states is identified.

DOI: 10.1103/PhysRevA.66.053615

PACS number(s): 03.75.Be, 42.50.Vk, 03.65.Xp, 05.45.Mt

Atom-optics experiments recently have been used to investigate the effect of underlying classical chaos on quantum dynamics. The experiments we focus on in this paper have demonstrated the existence of dynamic tunneling in momentum space in regimes where the underlying classical phase space contains a mixture of chaotic and regular orbits. We will show that we can accurately reproduce the dominant tunneling frequencies observed in these two very different experiments using Floquet analysis of the quantum dynamics.

Typically, cold sodium or cesium atoms are allowed to interact with laser beams that are detuned away from resonance with two atomic energy levels which have energy spacing,  $\hbar\omega_0$ . Two counterpropagating laser beams create a periodically modulated standing wave of light which stimulates absorption and then emission of a photon. This results in a net atomic recoil of  $2\hbar k_L$ , where  $k_L = \omega_L/c$  is the wave vector of the laser beams and  $\hbar$  is Planck's constant. When the laser detuning  $\delta_L = \omega_0 - \omega_L$  is large, this process dominates the dynamics.

A theoretical model which describes the atomic dynamics in such systems was developed by Graham, Schlautmann, and Zoller [1]. Recently, two groups (Steck, Oskay, and Raizen [2,3] in Texas and Hensinger *et al.* at NIST [4]) have performed independent experiments in which dynamic tunneling has been observed. In this paper, we explore the accuracy of the models used to analyze these experiments and the dynamical origin of the tunneling observed in each experiment. We first discuss the Texas experiment and then the NIST experiment.

In the Texas experiment [2,3], the dynamics of noninteracting cold cesium atoms, in an amplitude-modulated standing wave of light, was measured. The atomic center-of-mass Hamiltonian (in S.I. units) used to model dynamics of the cesium atoms is

$$\hat{H} = \frac{\hat{p}^2}{2m} - 2V_o \cos^2\left(\frac{\omega_m t}{2}\right) \cos(2k_L \hat{x}), \quad (1)$$

where  $\hat{p}$ ,  $\hat{x}$ , and  $m$  are the momentum, position, and mass, respectively, of a cesium atom,  $\omega_m = 2\pi/T$  is the modulation frequency, and  $V_o = \hbar\Omega_{\max}^2/8\delta_L$  is the ac Stark shift amplitude, where  $\Omega_{\max} = -2E_0 d/\hbar$  is the Rabi frequency,  $E_0$  is the electric-field strength, and  $d$  is the dipole moment of cesium [5].

In the experiments, the initial state is well localized at discrete momentum states separated by  $2\hbar k_L$ . This quantization of the momentum occurs naturally in the experiment due to the presence of counterpropagating laser beams which cause two-photon transitions. Therefore, in our theoretical analysis, we perform a scaling which explicitly quantizes the momentum in units of  $2\hbar k_L$ . As we will see later, this allows us to use Floquet theory rather than Floquet-Bloch theory, which deals with a continuum of momentum states [6]. Let  $\hat{\phi} = 2k_L \hat{x}$ ,  $\hat{p} = 2\hbar k_L \hat{p}$ ,  $\omega_r = \hbar k_L^2/2m$ ,  $\omega = \omega_m/4\omega_r$ ,  $t' = 4\omega_r t$ , and  $\hat{H}_{\text{theor}} = m\hat{H}/2k_L^2\hbar^2$ , to obtain

$$\hat{H}_{\text{theor}} = \hat{n}^2 - \frac{\alpha\omega^2}{8\pi^2} \left[ \cos(\hat{\phi}) + \frac{1}{2}\cos(\hat{\phi} - \omega t') + \frac{1}{2}\cos(\hat{\phi} + \omega t') \right], \quad (2)$$

where  $\alpha = 8\omega_r T^2 V_o/\hbar$ . All quantities are dimensionless and  $\hat{n}$  is the dimensionless momentum operator with eigenstates,  $|n\rangle$ , and integer eigenvalues,  $-\infty \leq n \leq \infty$ . [Note that the experimental papers [2,3] perform the scaling  $\hat{\phi} = 2k_L \hat{x}$ ,  $\tau = \omega_m t/2\pi = t/T$ ,  $\hat{\rho} = 4\pi k_L \hat{p}/m\omega_m$ ,  $\hat{H}_{\text{exp}} = 16\pi^2 k_L^2 \hat{H}/m\omega_m^2$ , and the Hamiltonian takes the form  $\hat{H}_{\text{exp}} = (\hat{\rho}^2/2) - 2\alpha \cos^2(\pi\tau) \cos(\hat{\phi})$ .] This system has three primary resonances centered at  $(n=0, \phi=0)$  and  $(n=\pm\omega/2, \phi=0)$ . For small values of  $\alpha$  ( $\alpha < 1.5$ ), the primary resonances have pendulumlike structure, and the resonance at  $n=0$  has half-width  $\Delta n_0 = \sqrt{\alpha\omega^2/4\pi^2}$ , while the resonances at  $n_{\pm} = \pm\omega/2$  have half-width  $\Delta n_{\pm} = \Delta n_0/\sqrt{2}$  [7]. The primary resonance at  $n=0$  bifurcates at  $\alpha \approx 7.0$ . The two outer primaries remain visible until  $\alpha \approx 13.0$ , when they disappear.

The classical motion is obtained from Hamilton's equations,  $\dot{n} = -\partial H_{\text{theor}}/\partial\phi$  and  $\dot{\phi} = \partial H_{\text{theor}}/\partial n$ . In the Texas experiment,  $\omega_r = 1.30 \times 10^4$  rad/s and  $T = 2\pi/\omega_m = 20 \mu\text{s}$ , which, for small  $\alpha$ , gives a location of  $n_{\pm} = \pm 3.0$  for the outer primary resonances. For the field strength  $\alpha = 9.7$ , used in the Texas experiment, the pendulum approximation for the half-widths of the two outer primary resonances gives  $\Delta n_{\pm} = 2.1$ , while the half-width of the central island is  $\Delta n_0 = 3.0$ . Thus the Texas experiment, for  $\alpha = 9.7$ , is in the strong field regime, where the primary resonances have overlapped and considerable chaos is expected [7]. A surface of

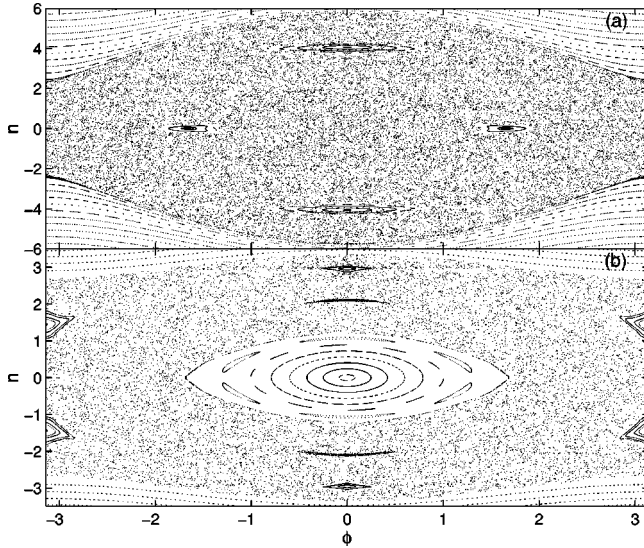


FIG. 1. Classical strobe plots. (a) The Texas experiment with  $\omega=6.0$  and  $\alpha=9.7$ . (b) The NIST experiment with  $\omega=2.5$ ,  $\alpha=1.66$ , and  $\epsilon=0.29$ .

section of the classical phase space for  $\alpha=9.7$  is shown in Fig. 1(a). The central primary resonance has bifurcated and is largely destroyed, and the outer primary resonances have been reduced significantly in size and are centered at momentum values  $n=\pm 4.2$ . Note also that the chaotic region lies in the interval  $-5\leq n\leq +5$ , indicating that eleven quantized momentum states determine the dynamics in the chaotic region.

The Texas experiment used atoms prepared initially with a narrow momentum distribution peaked at  $n=4.2$  (on the upper island). To numerically simulate this initial condition, we solved the Schrödinger equation,  $i[\partial|\Psi(t')\rangle/\partial t'] = \hat{H}_{\text{theor}}|\Psi(t')\rangle$ , using momentum states,  $|n\rangle$ , as a basis. A coherent state,

$$\begin{aligned} \langle n|\Psi(0)\rangle &\equiv \langle n|\phi_o n_o\rangle \\ &= \left(\frac{\sigma^2}{\pi}\right)^{1/4} \exp\left[\frac{-\sigma^2}{2}(n-n_o)^2 - i(n-n_o)\phi_o\right], \end{aligned} \quad (3)$$

centered at  $(n=n_o, \phi=\phi_o)$  is used as the initial state, with  $\sigma=1.2$ , which was used in the experiment. In the momentum basis, the Schrödinger equation reduces to a system of coupled first-order differential equations for the amplitudes,  $\langle n|\Psi(t)\rangle$ . This system was truncated, and 81 equations for the states  $\langle n|\Psi(t)\rangle$  with  $-40\leq n\leq 40$  were kept. The time variation of the average momentum,  $\langle n\rangle$ , is shown in Figs. 2(a), 2(b), and 2(c) for  $\alpha=8.0, 9.7$ , and  $13.0$ , respectively. In all cases, the initial state is  $(n_o=4.2, \phi_o=0)$ . For all three plots, the average momentum oscillates between the outer primary resonances. The plot for  $\alpha=8.0$  ( $\alpha=9.7$ ) has two dominant frequencies,  $f_1=1.95$  kHz and  $f_2=2.73$  kHz ( $f_1=2.39$  kHz and  $f_2=2.88$  kHz), giving rise to a beating effect. The beating effect at  $\alpha=9.7$  was observed in the Texas

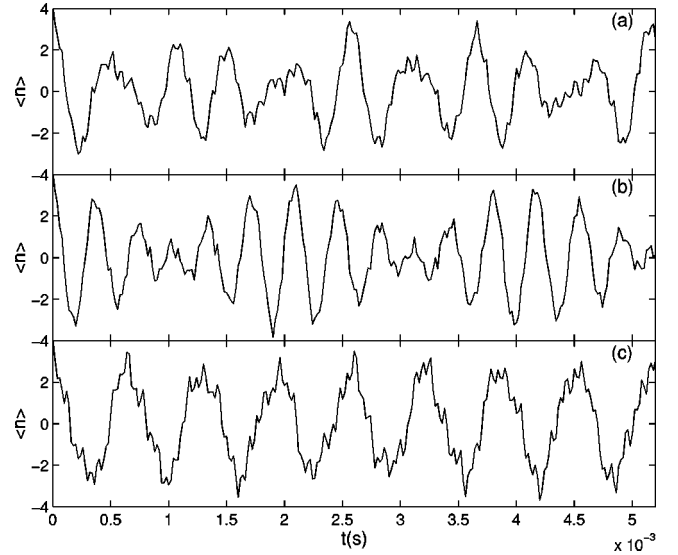


FIG. 2. Evolution of average momentum,  $\langle n\rangle$  (in dimensionless units), for the Texas experiment for  $\omega=6.0$ : (a)  $\alpha=8.0$ , (b)  $\alpha=9.7$ , and (c)  $\alpha=13.0$ .

experiment [3], but the experimental error bars were too great to resolve it at  $\alpha=8.0$ . The plot for  $\alpha=13.0$  shows one dominant frequency,  $f=1.56$  kHz.

It is useful to examine these results using Floquet theory [7]. Because the Hamiltonian  $\hat{H}_{\text{theor}}$  has time periodic coefficients, the Schrödinger equation has Floquet solutions of the form  $\langle n|\Psi(t)\rangle = e^{-i\Omega_j t} \langle n|\chi_j(t)\rangle$ , where  $\Omega_j$  is the  $j$ th Floquet eigenphase, and  $|\chi_j(t)\rangle$  is the  $j$ th Floquet eigenstate and is periodic in time,  $|\chi_j(t)\rangle = |\chi_j(t+T)\rangle$  [7]. The Floquet eigenphases  $\Omega_j$  are conserved quantities, and the eigenstates form a complete orthonormal basis which can be used to analyze the dynamics. The states  $|\chi_j(0)\rangle$  are eigenfunctions of the Floquet matrix,  $\hat{U}(T)$ , and the phase functions  $e^{-i\Omega_j T}$  are its eigenvalues. The Floquet matrix is computed by taking a momentum eigenstate as the initial state and evolving it for one period  $T$  using the Schrödinger equation. The resulting vector (in the momentum basis) is a column of the Floquet matrix.

The overlap probabilities  $P_j \equiv |\langle \chi_j(0)|\phi_o n_o(0)\rangle|^2$  give the contribution of each Floquet state to the dynamics. The probability to find the system in momentum state,  $|n\rangle$ , at time  $t$  can be written [7]

$$\begin{aligned} |\langle n|\phi_o n_o(t)\rangle|^2 &= \sum_i \sum_j \exp(-i(\Omega_j - \Omega_i)t) \\ &\quad \times \langle n|\chi_j(t)\rangle \langle \chi_i(t)|n\rangle \langle \chi_j(0)|\phi_o n_o(0)\rangle \\ &\quad \times \langle \phi_o n_o(0)|\chi_i(0)\rangle, \end{aligned} \quad (4)$$

with time  $t$  in seconds and  $\Omega_j/2\pi$  in Hertz. The oscillation frequencies  $f_{\text{exp}}$  observed in the experiments can be equated to differences between Floquet eigenphases. The frequency differences  $f_{\text{exp}} = (\Omega_j - \Omega_i)/2\pi$  for Floquet eigenstates with overlap probability,  $P_i P_j \geq 0.04$ , are plotted in Fig. 3 for the range of parameters shown in the Texas experiment [3]. Each

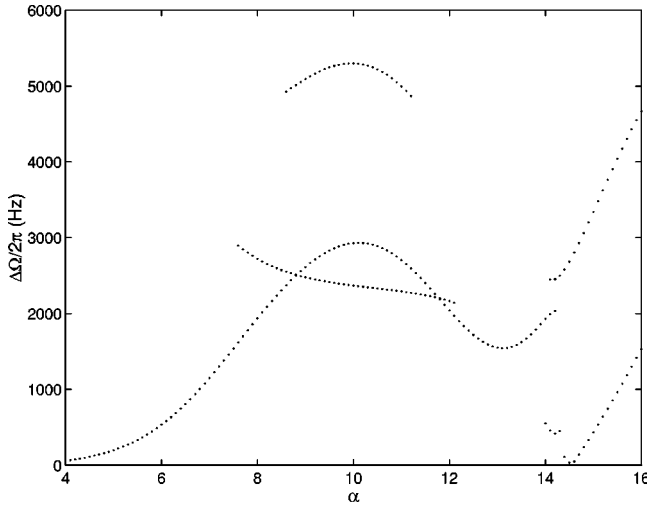


FIG. 3. Oscillation frequencies,  $\Delta\Omega = (\Omega_j - \Omega_i)$ , calculated from the Floquet eigenphase differences for varying dimensionless field strengths,  $\alpha$ . A threshold of  $P_i P_j \geq 0.04$  overlap probability was used to select the dominant frequencies. The three values shown at  $\alpha = 9.7$  correspond to  $(\Omega_{4a} - \Omega_{4b})/2\pi$ ,  $(\Omega_{4a} - \Omega_{4c})/2\pi$ , and  $(\Omega_{4b} - \Omega_{4c})/2\pi$ .

curve is a plot of the frequency difference between two Floquet states as a function of  $\alpha$ . At values of  $\alpha$  where there are multiple curves, there are more than two dominant frequencies. The Texas experiment was able to resolve the dominant frequencies,  $f_{\text{exp}} < 3$  kHz, in the interval between  $\alpha \approx 8.7$  and  $\alpha \approx 10.3$ . Our analysis exactly reproduces those experimental results. In the amplitude range  $\alpha \approx 7.6$  to  $\alpha \approx 11.6$ , we find that two frequencies dominate and give rise to the beats seen in Figs. 2(a) and 2(b). In the Texas data [3], large error bars occur in the regions  $\alpha \leq 7.0$  and  $\alpha \geq 13.7$ . This may be due to the rapid change in the dominant frequencies in those regions. A fundamental change in the dynamics occurs for  $\alpha > 14$ , where a different set of Floquet states begins to dominate the dynamics.

Only 11 Floquet states have support on momentum in the region  $n = -5$  to  $n = 5$ , and determine the dynamics in the chaotic region. In Figs. 4(a)–4(d), we show Husimi plots for the Floquet states which, for  $\alpha = 9.7$ , have the largest overlap probability, three of which dominate the dynamics. The dark regions of these plots show the region of the classical phase space where the probability of finding the cesium atoms is largest. The eigenphase differences  $(\Omega_{4b} - \Omega_{4a})/2\pi = 2.89$  kHz and  $(\Omega_{4a} - \Omega_{4c})/2\pi = 2.40$  kHz correspond to the two dominant oscillation frequencies observed by the Texas experiment at  $\alpha = 9.7$ . The state in Fig. 4(d) has the fourth highest overlap probability,  $P_d = 0.045$ , but it lies in the chaotic sea. The state in Fig. 4(d) and others not shown contribute to the fine scale structure in these curves.

Let us now consider the NIST experiment [4], which used a Bose-Einstein condensate of sodium atoms to observe dynamic tunneling. Formation of a condensate with the sodium atoms yields a narrower distribution of initial momenta than the Texas experiment. The Hamiltonian used to describe the experiment can be written in the form

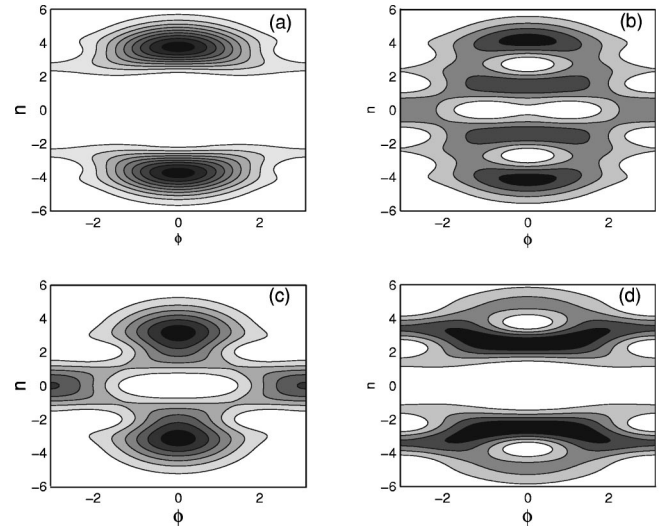


FIG. 4. Husimi plots of Floquet eigenstates for the Texas experiment for  $\omega = 6.0$  and  $\alpha = 9.7$ . (a) Floquet eigenphase  $\Omega_{4a}/2\pi = 16.9$  kHz and an overlap probability  $P_{4a} = 0.416$ . State (b) Floquet eigenphase  $\Omega_{4b}/2\pi = 19.7$  kHz and an overlap probability  $P_{4b} = 0.224$ . (c) Floquet eigenphase  $\Omega_{4c}/2\pi = 14.5$  kHz and an overlap probability  $P_{4c} = 0.20$ . (d) Floquet eigenphase  $\Omega_{4d}/2\pi = 18.4$  kHz and an overlap probability  $P_{4d} = 0.045$ .

$$\hat{H}_{\text{theor}} = \hat{n}^2 + \frac{\tilde{\omega}^2 \kappa}{2} [1 + 2\nu \epsilon \cos(\tilde{\omega} t') - \cos \hat{\phi} - \nu \epsilon \cos(\hat{\phi} - \tilde{\omega} t') - \nu \epsilon \cos(\hat{\phi} + \tilde{\omega} t')], \quad (5)$$

where  $\nu = \pm 1$ . When  $\nu = +1$  ( $\nu = -1$ ), Eq. (5), with starting time  $t' = 0$ , reproduces the dynamics of the NIST experiment, which has starting time  $\tilde{\tau} = T/4$  ( $\tilde{\tau} = 3T/4$ ). This Hamiltonian again discretizes the momentum in units of  $2\hbar\tilde{k}_L$ , which reflects the quantization of momentum due to the two-photon transitions. (The Hamiltonian  $\hat{H}_{\text{exp}} = (\hat{\rho}^2/2) + 2\kappa [1 + 2\epsilon \sin(\tilde{\omega}_m \tilde{\tau})] \sin^2(\hat{\phi}/2)$  used in the experimental paper is obtained by setting  $\hat{\rho} = (4\hbar\tilde{k}_L^2/m\tilde{\omega}_m)\hat{n}$  and  $\hat{H}_{\text{exp}} = (8\tilde{k}_L^4\hbar^2/m^2\tilde{\omega}_m^2)\hat{H}_{\text{theor}}$ .)

For small amplitudes,  $\kappa$  and  $\kappa\epsilon$ , the NIST Hamiltonians have three primary resonances. For  $\nu = -1$ , they are located at  $(n=0, \phi=0)$  and  $(n = \pm\tilde{\omega}/2, \phi = \pm\pi)$ , while for  $\nu = +1$  they are located at  $(n=0, \phi=0)$  and  $(n = \pm\tilde{\omega}/2, \phi = 0)$ . They have half-widths,  $\Delta n_0 = \sqrt{\tilde{\omega}^2 \kappa}$  and  $\Delta n_{\pm} = \sqrt{\tilde{\omega}^2 \kappa \epsilon}$  [7].

A strobe plot of the classical phase space for the Hamiltonian in Eq. (5) with  $\nu = -1$  and experimental parameters  $\tilde{\omega}_m/2\pi = 250$  kHz,  $\tilde{\omega} = 2.5$ ,  $\kappa = 1.66$ , and  $\epsilon = 0.29$  is shown in Fig. 1(b). Seven Floquet states determine the dynamics in the chaotic region between  $n = -3$  and  $n = 3$ . For the parameters used in the experiment, the pendulum approximation predicts the primary resonances to lie at  $n=0$  and to  $n = \pm 1.25$ , and have half-widths  $\Delta n_0 = 3.2$  and  $\Delta n_{\pm} = 1.7$ . We find that the primary resonances are totally destroyed at  $\kappa \approx 0.2$ , and then new resonances, which resemble the primaries, reappear and disappear repeatedly as  $\kappa$  is increased. For

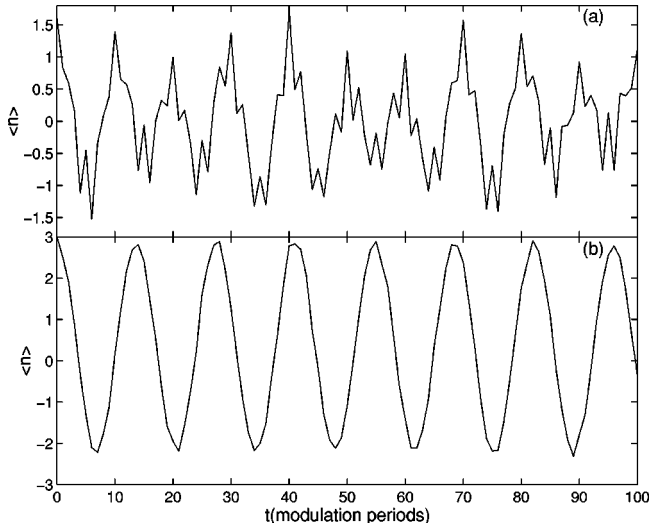


FIG. 5. Evolution of momentum expectation value,  $\langle n \rangle$  (in dimensionless units), for the NIST experiment for  $\kappa=1.66$ ,  $\epsilon=0.29$ ,  $\tilde{\omega}=2.5$ , and  $\tilde{\omega}_m/2\pi=250$  Hz: (a)  $n_o=1.6$  and  $\phi_o=0$ ; (b)  $n_o=3.0$  and  $\phi_o=0$ .

$\kappa=1.66$  and  $\epsilon=0.29$ , a large resonance exists at  $(n=0, \phi=0)$  and three small pairs of higher-order resonances exist at  $(n \approx \pm 1.5, \phi = \pm \pi)$ ,  $(n \approx \pm 3.0, \phi=0)$ , and  $(n \approx \pm 2.0, \phi=0)$ .

In Fig. 5, we show the time evolution of the momentum expectation value for two different initial conditions for the  $\nu=-1$  Hamiltonian at parameter values,  $\kappa=1.66$ ,  $\epsilon=0.29$ ,  $\tilde{\omega}=2.5$ , and  $\tilde{\omega}_m/2\pi=250$  kHz. Figure 5(a), with  $(n_o=1.6, \phi_o=0)$ , shows a somewhat noisy oscillation with a dominant frequency 24.9 kHz (10.0 modulation periods), which is in good agreement with the experimental result. Figure 5(b) shows the case with  $(n_o=3.0, \phi_o=0)$ . A clean oscillation with frequency 18.3 kHz (13.7 modulation periods) occurs. This oscillation was not observed in the experiment, but we expect it would show up in a power spectrum of the experimental data.

We now consider a Floquet analysis for both Hamiltonians,  $\nu=\pm 1$ . The Floquet eigenphases for  $\nu=\pm 1$  are identical, but the Floquet eigenstates associated with each eigenphase are different for the two Hamiltonians. Let us first consider the  $\nu=-1$  Hamiltonian with parameters,  $\kappa=1.66$ ,  $\epsilon=0.29$ ,  $\tilde{\omega}=2.5$ , and  $\tilde{\omega}_m/2\pi=250$  kHz. In Figs. 6(a) and 6(b), we show the two Floquet states which dominate the dynamics for initial condition,  $(n_o=1.6, \phi_o=0)$ . They have a frequency difference  $(\Omega_{6b}-\Omega_{6a})/2\pi=25.0$  kHz. Their frequency difference accounts for the oscillation of 10 modulation periods reported in [4]. These Floquet states are not even-odd pairs as suggested in [4], and they both lie in the chaotic sea. If the effective Planck's constant for this experiment were smaller, more Floquet states would be supported by the chaotic region and we would not expect to find this simple oscillation [8] for this initial condition.

If we take the initial condition  $(n_o=3.0, \phi_o=0)$  for  $\nu=-1$ , we obtain the oscillation shown in Fig. 5(b). This

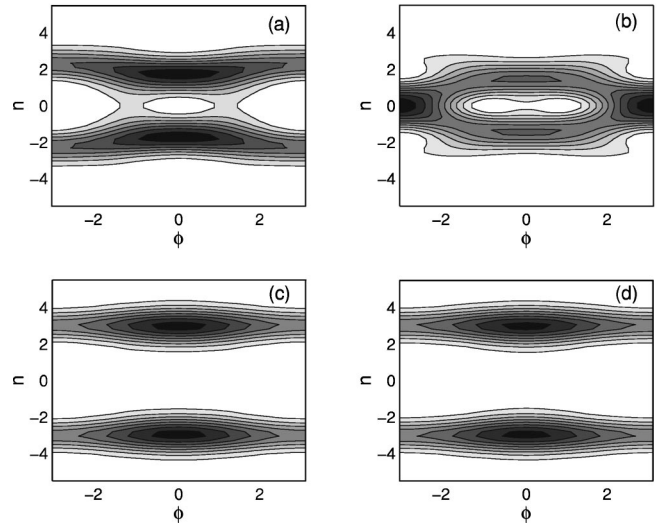


FIG. 6. Husimi plots of Floquet eigenstates for the NIST experiment with  $\kappa=1.66$ ,  $\epsilon=0.29$ ,  $\tilde{\omega}=2.5$ , and  $\tilde{\omega}_m/2\pi=250$  Hz. (a) Floquet eigenphase  $\Omega_{6a}/2\pi=49.0$  kHz and overlap probability  $P_{6a}=0.380$ . State (b) Floquet eigenphase  $\Omega_{6b}/2\pi=73.9$  kHz and overlap probability  $P_{6b}=0.306$ . (c) Floquet eigenphase  $\Omega_{6c}/2\pi=15.3$  kHz and overlap probability  $P_{6c}=0.427$ . (d) Floquet eigenphase  $\Omega_{6d}/2\pi=33.5$  kHz and overlap probability  $P_{6d}=0.421$ .

oscillation results from the even-odd Floquet pair shown in Figs. 6(c) and 6(d). Figure 6(c) [Fig. 6(d)] is even (odd) under the transformation  $n \rightarrow -n$ . They have a frequency difference  $(\Omega_{6c}-\Omega_{6d})/2\pi=18.3$  kHz. This oscillation appears to result from states sitting in the outermost nonlinear resonance.

We finally consider the  $\nu=+1$  Hamiltonian with parameters  $\kappa=1.66$ ,  $\epsilon=0.29$ ,  $\tilde{\omega}=2.5$ , and  $\tilde{\omega}_m/2\pi=250$  kHz. We find that the 25.0 kHz (10 modulation periods) oscillation dominates those initial momentum states which are centered at  $\phi=0$  and lie in the interval  $n_o=1.7$  to  $n_o=3.0$ . These oscillations appear to result from the two Floquet states which lie in the chaotic sea. If we change the parameters to  $\kappa=1.82$  and  $\epsilon=0.30$  and the modulation frequency to  $\tilde{\omega}_m=222$  kHz, the dominant frequency for the initial state  $(n_o=2.0, \phi_o=0)$  is 36.8 kHz (6.03 modulation periods), which is in agreement with the NIST experiment.

In conclusion, the model Hamiltonians, with momentum quantized in units of  $2\hbar k_L$ , give extremely good predictions of the experimental results. Because of the momentum quantization imposed by the dynamics of the experiment, we found that it was advantageous to use Floquet theory rather than Floquet-Bloch theory to analyze the experiment. In fact, our results are so good that these models might be used to help calibrate future experiments.

The authors wish to acknowledge the Welch Foundation, Grant No. F-1051, NSF Grant INT-9602971, and DOE contract No. DE-FG03-94ER14405 for partial support of this work. We also thank the University of Texas at the Austin High Performance Computing Center for use of their computer facilities, and we thank Mark Raizen, Dan Steck, Wendell Oskay, and Chris Helmerson for useful conversations.

- [1] R. Graham, M. Schlautmann, and P. Zoller, *Phys. Rev. A* **45**, R19 (1992).
- [2] Daniel A. Steck, Windell H. Oskay, and Mark G. Raizen, *Science* **293**, 274 (2001).
- [3] Daniel A. Steck, Windell H. Oskay, and Mark G. Raizen, *Phys. Rev. Lett.* **88**, 120406 (2002).
- [4] W.K. Hensinger, H. Haeffner, A. Browaeys, N.R. Heckenberg, K. Helmerson, C. McKenzie, G.J. Milburn, W.D. Phillips, S.L. Rolston, H. Rubinsztein-Dunlop, and B. Upcroft, *Nature (London)* **412**, 52 (2001).
- [5] Daniel A. Steck, Valery Milner, Windell H. Oskay, and Mark G. Raizen, *Phys. Rev. E* **62**, 3461 (2000).
- [6] A. Mouchet, C. Miniatura, R. Kaiser, B. Gremaud, and D. Delande, *Phys. Rev. E* **64**, 016221 (2001).
- [7] L. E. Reichl, *Transition to Chaos in Conservative Classical Systems: Quantum Manifestations* (Springer-Verlag, New York, 1992).
- [8] Todd Timberlake and L.E. Reichl, *Phys. Rev. A* **59**, 2886 (1999).